

# Nanoscale

Accepted Manuscript



This is an *Accepted Manuscript*, which has been through the Royal Society of Chemistry peer review process and has been accepted for publication.

*Accepted Manuscripts* are published online shortly after acceptance, before technical editing, formatting and proof reading. Using this free service, authors can make their results available to the community, in citable form, before we publish the edited article. We will replace this *Accepted Manuscript* with the edited and formatted *Advance Article* as soon as it is available.

You can find more information about *Accepted Manuscripts* in the [Information for Authors](#).

Please note that technical editing may introduce minor changes to the text and/or graphics, which may alter content. The journal's standard [Terms & Conditions](#) and the [Ethical guidelines](#) still apply. In no event shall the Royal Society of Chemistry be held responsible for any errors or omissions in this *Accepted Manuscript* or any consequences arising from the use of any information it contains.



## Application of a SERS-based Lateral Flow Immunoassay Strip for Rapid and Sensitive Detection of Staphylococcal Enterotoxin B

Joonki Hwang,<sup>†</sup> Sangyeop Lee<sup>†</sup> and Jaebum Choo<sup>\*</sup>

Received 00th January 20xx,  
Accepted 00th January 20xx

DOI: 10.1039/x0xx00000x

www.rsc.org/

A novel surface-enhanced Raman scattering (SERS)-based lateral flow immunoassay (LFA) biosensor was developed to resolve problems associated with conventional LFA strips (e.g., limits in quantitative analysis and low sensitivity). In our SERS-based biosensor, Raman reporter-labeled hollow gold nanospheres (HGNs) were used as SERS detection probes instead of gold nanoparticles. With the proposed SERS-based LFA strip, the presence of a target antigen can be identified through a colour change in the test zone. Furthermore, highly sensitive quantitative evaluation is possible by measuring SERS signals from the test zone. To verify the feasibility of the SERS-based LFA strip platform, an immunoassay of staphylococcal enterotoxin B (SEB) was performed as a model reaction. The limit of detection (LOD) for SEB, as determined with the SERS-based LFA strip, was estimated to be 0.001 ng/mL. This value is approximately three orders of magnitude more sensitive than that achieved with the corresponding ELISA-based method. The proposed SERS-based LFA strip sensor shows significant potential for the rapid and sensitive detection of target markers in a simplified manner.

### Introduction

Lateral flow assay (LFA) strip biosensors are simple devices intended to detect the presence of a target analyte in a given sample. The benefits of LFA biosensors include short times to obtain test results, a user-friendly format, low cost, and long-term stability.<sup>1-3</sup> Consequently, LFAs have been extensively used in point-of-care (POC) tests, home tests, infectious disease diagnosis, and field tests for various hazardous materials in foods and environmental samples.<sup>4</sup> Colloidal gold nanoparticles are the most commonly used labels in LFA sensors because they are red in colour due to localized surface plasmon resonance.<sup>5-7</sup> In a typical testing procedure, the mobile phase is first pulled through the stationary phase by capillary action. The mobile phase then passes through a capture zone, where trapped labels, e.g., antibody-conjugated nanoparticles, accumulate in concentration until they are visually detectable. Indeed, such a test does not require any sample preparation or electronic devices, and only relies on visual detection. While LFA sensors have been successfully utilized in numerous sensing applications, they possess major limitations in terms of quantitative analysis and detection sensitivity.<sup>8,9</sup> Therefore, it is critical that steps be taken to enhance both the sensitivity and quantification capabilities of

LFA sensors.

Two factors can be considered to improve the sensitivity and quantification capability of LFA sensors in the detection of target analytes: the use of different detection labels and the employment of optical strip readers. Since the detection limit is closely related to the labels utilized for detection, alternative labels such as magnetic particles,<sup>10,11</sup> carbon nanoparticles,<sup>12,13</sup> fluorescence microspheres,<sup>14</sup> quantum dots,<sup>15-17</sup> up-converting phosphors,<sup>18,19</sup> and europium nanoparticles<sup>20,21</sup> have been used to improve sensor capabilities. In addition, corresponding optical strip readers for the detection of fluorescence, magnetic signals, electrochemical signals, and chemiluminescence signals have been employed for the quantification of target analytes.<sup>22</sup> In the case of gold nanoparticles, qualitative analysis can be conducted through a visual inspection of colours, but optical readers should be employed to measure the intensity of the colours produced in a test. The selection of a strip reader is mainly determined by the label employed in the analysis. Nonetheless, most of the detection methods described above still suffer from poor sensitivity and low precision.

In the present work, a conceptually new surface-enhanced Raman scattering (SERS)-based LFA sensor is introduced for the highly sensitive and rapid analysis of target analytes. The SERS-based immunoassay technique using antibody-conjugated gold nanoparticles has recently attracted significant attention due to its high sensitivity.<sup>23-29</sup> In the proposed SERS-based LFA strip sensor, all of the measurement principles are identical to those of a conventional POC LFA strip, with the exception of the detection nanoprobe. Instead of the gold nanospheres utilized in conventional POC LFA strips, Raman reporter-labelled hollow gold nanospheres

Department of Bionano Technology, Hanyang University, Ansan 426-791, South Korea. Telephone: +82-31-400-5201; Fax: +82-31-436-8188; E-mail: jchoo@hanyang.ac.kr

<sup>†</sup> These authors contributed equally to this work.

<sup>\*</sup> Corresponding author

Electronic Supplementary Information (ESI) available: [details of any supplementary information available should be included here]. See DOI: 10.1039/x0xx00000x

(HGNs)<sup>30-33</sup> were employed in this work as SERS nanoprobcs. Using the SERS-based LFA strip platform, the presence of target analytes can be identified through a colour change in the test zone. Furthermore, it is possible to achieve a quantitative result by measuring the SERS signal intensity.

To evaluate detection sensitivity and quantitative analysis capability of the devised SERS-based LFA strip platform, an immunoassay of staphylococcal enterotoxin B (SEB) was performed as a model reaction. The National Institute of Allergy and Infectious Diseases includes SEB as one of the toxins on its Biodefense Priority Pathogens list, which details agents for which sensitive and rapid detections are urgently needed.<sup>34,35</sup> SEB belongs to a family of heat-stable enterotoxins, and the amount of SEB to cause intoxication is less than 1 ng/mL. In this report, we demonstrate the detection of low SEB concentrations at sub-ng/mL levels in solution using a novel SERS-based LFA strip sensor.

## Experimental

### Materials

Gold (III) chloride trihydrate (HAuCl<sub>4</sub>), tri-sodium citrate (Na<sub>3</sub>-citrate), dihydrolipoic acid (DHLLA), 1-ethyl,3-(3-dimethylaminopropyl)carbodiimide (EDC), 4-(4-maleimidophenyl)butyric acid N-succinimidyl ester (NHS), ethanolamine, cobalt (II) chloride (CoCl<sub>2</sub>), bovine serum albumin (BSA), polyvinylpyrrolidone (PVP), tris-EDTA buffer (TE buffer, pH 8.0), anti-staphylococcal enterotoxin B polyclonal antibody produced in rabbit (S9008, Rabbit anti-SEB), and anti-mouse IgG antibody produced in goat (mouse IgG) were purchased from Sigma-Aldrich (St. Louis, MO, USA). Surfactant G was procured from Fitzgerald (Concord, MA, USA) for use as a detergent. Malachite green isothiocyanate (MGITC) was purchased from the Invitrogen Corporation (Carlsbad, CA, USA). Anti-staphylococcal enterotoxin B monoclonal antibody produced in mouse (S222, Mouse anti-SEB) was procured from Santa Cruz Biotechnology (Santa Cruz, CA, USA). Recombinant enterotoxin type B for staphylococcus aureus (SEB) was purchased from Cusabio (Wuhan, China). The nitrocellulose (NC) membrane attached to a backing card (Hi-flow plus HF180) was purchased from the Millipore Corporation (Billerica, MA, USA). Absorbent pads (CF3) were procured from Whatman-GE Healthcare (Pittsburgh, PA, USA).

### Synthesis of hollow gold nanospheres and antibody conjugation

Hollow gold nanospheres (HGNs) were prepared according to a method detailed in previous reports.<sup>30-32</sup> Briefly, HGNs were synthesized by controlling the growth of reduced gold nanoshells around a cobalt nanoparticle. Cobalt nanoparticles were synthesized by reducing CoCl<sub>2</sub> with NaBH<sub>4</sub> under high purity N<sub>2</sub> gas purging conditions. Upon the addition of a HAuCl<sub>4</sub> solution, gold atoms were nucleated and eventually formed small shells around the cobalt nanoparticles. The cobalt was then completely dissolved, producing gold nanospheres with a hollow interior. HGNs were characterized by UV/Vis absorption spectroscopy, transmission electron

microscopy (TEM), and dynamic light scattering (DLS) measurements (Fig. S1). The average diameter and wall thickness of the HGNs were estimated to be 45 ± 12 nm and 15 ± 5 nm, respectively. A sequential procedure for the fabrication of SERS nano-tags has been reported elsewhere. Briefly, 5.0 μL of a 10 μM MGITC solution (Raman reporter) was added to 1.0 mL of a 0.1 nM HGN solution. The mixture was subsequently reacted for 30 min with stirring. The surface of the MGITC-labelled HGNs was modified using 0.1 μL of a 1.0 mM DHLA solution for 30 min. Activated carboxyl groups on the surface of the HGNs were then reacted with 1.0 μL of a 0.1 mM EDC/NHS solution for 1 h. Next, 0.1 μL of 1.0 mg/mL mouse anti-SEB was reacted with the solution for 1 h. Nonspecific binding chemicals and antibodies were removed by centrifugation, and then 0.5 μL of a 1.0 mM ethanolamine solution was added in order to deactivate unreacted sites on the surface of the HGNs. Finally, antibody-conjugated HGNs were stabilized at 4 °C. For efficient diffusion in the LFA strip, 20 μL of 10× antibody-conjugated HGNs were mixed with 20 μL of surfactant G (10%), 20 μL of PVP (10%), and 40 μL of TET buffer (Tween 20, 0.05 v/v%, pH 8.0).

### Preparation of LFA strip

The LFA strip is composed of four components: a sample loading pad, a conjugate pad, an NC membrane, and an absorbent pad. To fabricate the strip, the NC membrane with a 3~10 μm pore size was first attached to a plastic backing card, and an absorbent pad was affixed to its ending part. The test zone and control zone on the NC membrane were prepared by dispensing 0.5 mg/mL of rabbit anti-SEB and 0.1 mg/mL of mouse anti-IgG, respectively. Each antibody was sprayed onto the NC membrane at a rate of 0.5 μL/cm using a precision line dispensing system (Zeta Corporation, South Korea). The membrane was then dried for 1 h at room temperature. Strips with a 3.8 mm width were cut using a programmable cutter (Zeta Corporation, South Korea). Finally, the LFA strips were stored in a sealed falcon tube. To simplify the LFA sensing

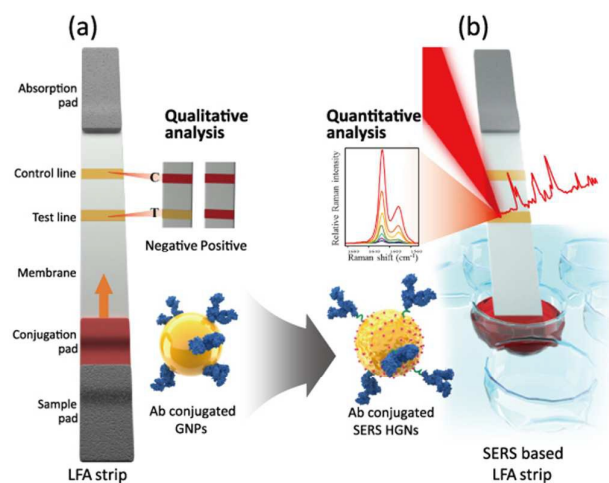


**Fig. 1** Schematic illustration of (a) a conventional LFA strip and (b) the SERS-based LFA strip. Only one red band is observed in the control zone in the absence of the target antigen (negative), while two red bands appear in the presence of the target antigen (positive). With the SERS-based LFA strip, highly sensitive quantification of target analytes is possible by monitoring the SERS peak intensity.

procedure, a 96-well ELISA plate was employed as the dipping substrate. Lateral diffusion through the strip was achieved by dipping the LFA strip into the sample solutions contained in each well.

### Instrumentation

Raman spectra and SERS mapping images for the test zone of the LFA strip were acquired using an In Via Renishaw Raman microscope system (Renishaw, New Mills, United Kingdom); a He–Ne laser with a power of 3 mW operating at  $\lambda=633$  nm was utilized as the excitation source. The Rayleigh line was removed from the collected Raman data by placing a holographic notch filter in the collection path. A charge-coupled device (CCD) camera was coupled to a spectrograph to provide a combined spectral resolution of  $1\text{ cm}^{-1}$ . Raman images were obtained using a Raman point-mapping method with a  $50\times$  objective lens. A computer-controlled  $x$ – $y$  translational stage was scanned in  $10\text{ }\mu\text{m} \times 10\text{ }\mu\text{m}$  steps over a  $200\text{ }\mu\text{m}$  ( $x$  axis) and  $800\text{ }\mu\text{m}$  ( $y$  axis) range (total 1,600 pixels). Data acquisition time at each pixel is 0.1 sec, and total image acquisition time is 6 min (3 min for imaging a test line and another 3 min for imaging a control line). The numerical aperture of the objective lens used in this work (N/A) is 0.75. The SERS images acquired for each strip were decoded using WiRE software V 4.0 (Renishaw, New Mills, United Kingdom) and the characteristic peak intensity of MGITC at  $1615\text{ cm}^{-1}$ . SERS spectra were quantitatively analyzed with WiRE software (Renishaw, New Mills, United Kingdom). A Cary 100 spectrophotometer (Varian, Salt Lake City, UT, USA) was used to acquire UV/visible absorption spectra. High-magnification transmission electron microscopy (TEM) images were obtained with a JEOL JEM 2100F instrument at an accelerating voltage of 200 kV. Scanning electron microscopy (SEM) images were acquired using a TESCAN (MIRA3) instrument at an accelerating voltage of 20 kV. Dynamic light scattering (DLS) data were obtained for the NPs with a Nano-ZS90 (Malvern) apparatus. An ELISA assay was performed using a microplate reader (Power Wave X340, Bio-Tek, Winooski, VT, USA) equipped with a 96-well plate. The phase contrast intensity in the test zone was measured with a Chemi-Doc imaging system (Bio-Rad, Hercules, California, USA).

### Results and discussion

The operating principle of the SERS-based LFA strip is based on sandwich-type antibody/antigen/antibody-conjugated HGN reactions. Fig. 1a illustrates the configuration and measurement principle of a conventional LFA strip. In a typical assay, the sample solution containing target antigens is applied onto the sample pad. The solution then migrates by capillary action and passes through the conjugation pad, at which point immuno-reactions between the target antigens and antibody-conjugated gold nanoparticles occur. The immunocomplexes (antigens/gold nanoparticles) continue to migrate along the membrane pad until they reach the test zone, where they are captured by a second immuno-reaction

with the antibodies immobilized in the test zone. The accumulation of gold nanoparticles produces a characteristic red band in the test zone. Excess antibody-conjugated gold nanoparticles continue to migrate and are captured by antibodies immobilized in the control zone. Finally, two red bands appear in the presence of the target antigen (positive), whereas only one red band is observed in the control zone when no target antigen is present (negative). A red band in the control zone means that the LFA strip is working properly.

While LFA strips have been successfully utilized in numerous point-of-care applications, including acute and chronic disease detection, they possess major limitations when high sensitivity is required. Such a drawback is especially critical in the early diagnosis of diseases. Furthermore, it is impossible to acquire quantitative information when using an LFA strip. To resolve these issues, SERS-based LFA strips were developed in this work. The combination of highly sensitive SERS detection with existing LFA strip sensor technology is considered to be an ideal sensing platform to overcome the low sensitivity problem in various commercialized point-of-care LFA strip sensors. Fig. 1b displays a schematic of the sensing platform for the SERS-based LFA strip. The measurement principles are identical to those of a conventional LFA strip, except that antibody-conjugated nanoparticles are utilized. In the SERS-based LFA strip, Raman reporter-labelled HGNs were used as SERS detection probes for the quantitative evaluation of target antigens. The presence of target antigens can be confirmed through a colour change in the test zone. A quantitative evaluation of target antigens is also possible by measuring SERS signals. Here, the immobilization of antibodies on the HGN surface can affect their diffusion performance on the strip. Therefore, two different immobilization methods were tested; physical adsorption and covalent conjugation. Fig. S2 shows the DLS

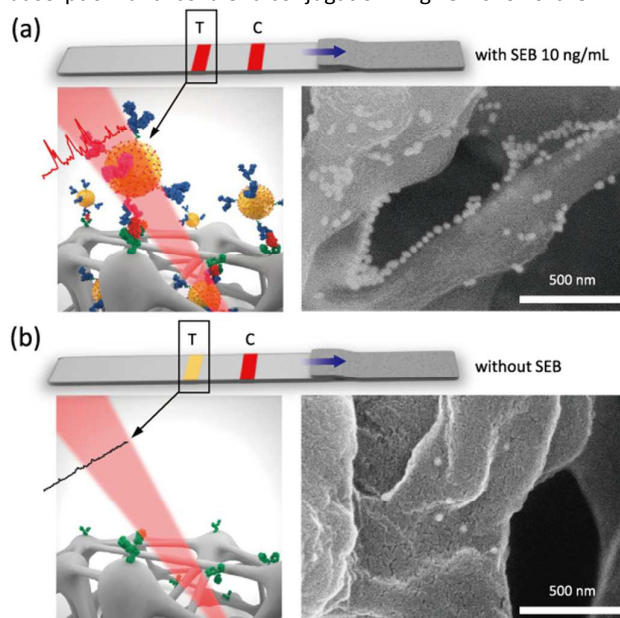


Fig. 2 SEM images obtained for HGN immunocomplexes (a) with 10 ng/mL of SEB and (b) without SEB in the test zone.

distributions for two different types of HGNs. Chemically conjugated HGNs (Fig. S2b) demonstrate a much narrower size distribution than physically adsorbed HGNs (Fig. S2a). In the case of chemical conjugation, the average diameter difference is estimated to be less than 10 nm, whilst that of physically adsorbed HGNs is over 70 nm. This huge change of average diameter size is caused by the aggregation of HGNs. Photographic images of the LFA strips in the middle of Fig. S2 indicate that chemically conjugated HGNs have a longer migration distance than physically adsorbed HGNs. As such, the former are more favourable for the formation of sandwich immunocomplexes on the LFA strip.

Fig. 2 displays SEM images obtained for HGN immunocomplexes in the test zone. When a target antigen (SEB) is present (10 ng/mL), a cluster of HGNs was observed in the paper fiber pores, as shown in Fig. 2a. This clustering is responsible for the color change to red ("On"), as well as the high SERS activity of the substrate. In the absence of SEB, no color change was observed ("Off") since no immunocomplexes are formed in the test zone; this is evident in Fig. 2b. In this case, no SERS activity was apparent on the substrate either. Consequently, the presence of target antigens can be identified by the naked eye, as in a conventional LFA strip. However, in the SERS-based LFA strip, a quantitative analysis of target antigens is also possible by measuring the characteristic Raman signal of the SERS nanoprobes.

Fig. 3a shows the SERS mapping images obtained with a peak intensity at  $1615\text{ cm}^{-1}$  for different concentrations of SEB.

Here, images of  $80 \times 20$  pixels (1 pixel =  $10\text{ }\mu\text{m} \times 10\text{ }\mu\text{m}$ ) were collected for each concentration in the range of  $0 \sim 1000\text{ ng/mL}$ . The bar scale on the bottom left displays the color decoding scheme for the SERS intensity; a brighter color denotes a stronger SERS intensity. With an increase in the SEB concentration from  $0.1\text{ }\mu\text{g/mL}$  to  $1000\text{ ng/mL}$ , more sandwich immunocomplexes were formed on the substrate, leading to an increase in the SERS intensity. Consequently, the immobilized area of the HGN SERS probe became brighter with an increase in the SEB concentration. However, it is worth noting that the SERS signal intensity within the same  $80 \times 20$  pixel area is not homogeneous, indicating that the hot spots in each pixel are not uniform because of different conditions on the substrates. In most cases, it is difficult to achieve a highly homogeneous SERS mapping image even though the surface morphology and detection conditions are carefully controlled. To resolve this problem, the SERS signal intensities for 1600 pixel points were averaged so as to obtain a reproducible intensity value. In the majority of previous reports, about five to ten points were averaged in order to construct a calibration curve for quantitative evaluations. In this work, however, SERS imaging and averaging methods were employed for a highly reproducible analysis of SEB markers. Fig. 3b displays the average SERS spectra for 1600 pixel points of the SERS mapping zones (shown in Fig. 3a) in the presence of various SEB concentrations. The intensity of the Raman peaks increases concomitantly with an increase in the SEB concentration. SERS mapping images for the control region of

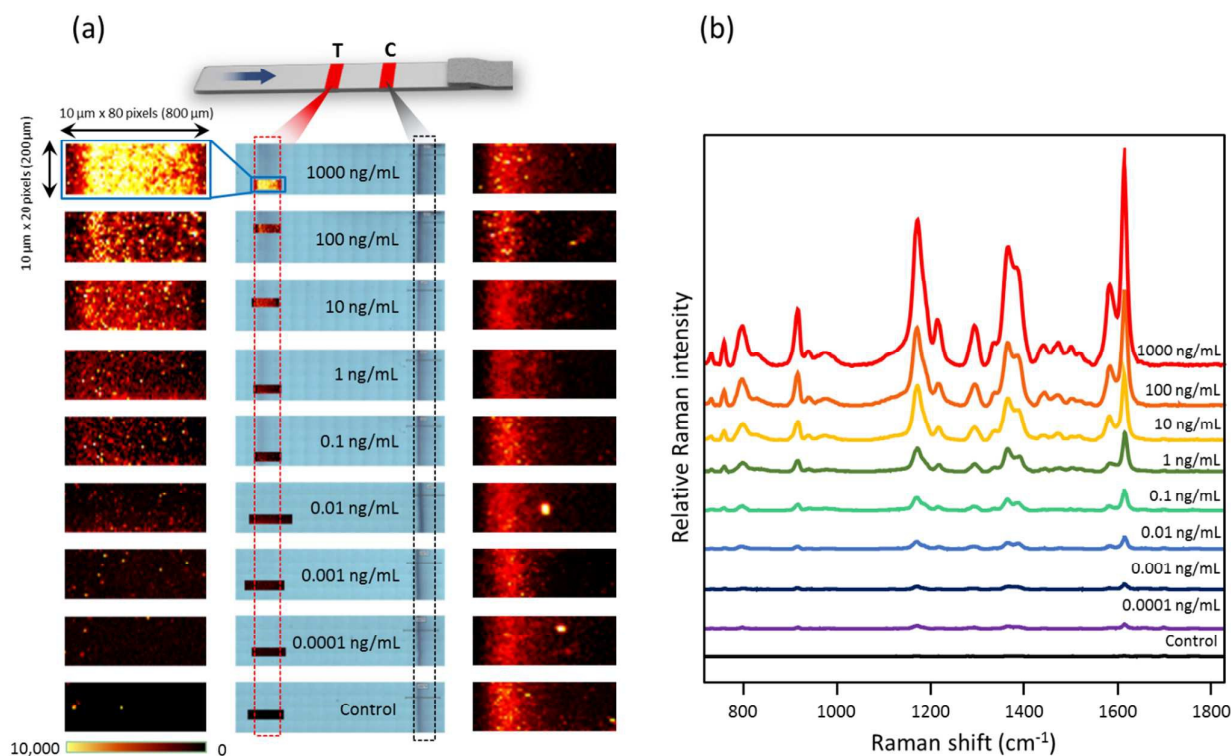


**Fig. 3** (a) SERS mapping images acquired using a peak intensity at  $1650\text{ cm}^{-1}$  for nine different SEB concentrations over a range of  $0.1\text{ }\mu\text{g/mL} \sim 1,000\text{ ng/mL}$ ;  $80 \times 20$  pixels (1 pixel =  $10\text{ }\mu\text{m} \times 10\text{ }\mu\text{m}$ ) were imaged for each concentration. The scale bar at the bottom displays the color decoding scheme for different SERS intensities. (b) Average SERS spectra for the 1600 pixel points of the SERS mapping zones.

the LFI strip were also measured, and it is confirmed that consistent SERS mapping images are observed for the control zone regardless of different SEB concentrations.

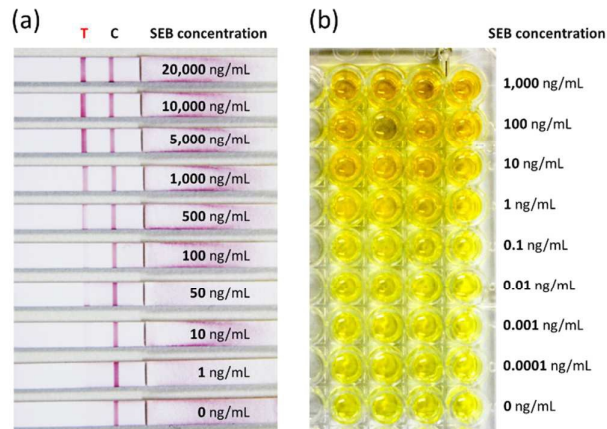


**Fig. 4** (a) Photographic image of the LFA strip after applying different concentrations of SEB from 1 ~ 20,000 ng/mL. Quantitative analysis was also performed by recording the intensities of the test zones using a Chemi-Doc imaging system. In the phase contrast analysis, the limit of detection (LOD) was determined to be 10 ng/mL. (b) ELISA analysis for various concentrations of SEB in a 96-well plate; the LOD was estimated to be 1.0 ng/mL.

To evaluate the detection sensitivity of the SERS-based LFA strip, POC-based LFA and ELISA immunoassay tests were performed. Sample solutions containing different concentrations of target SEB markers were tested under optimized experimental conditions. First, 20  $\mu$ L of the SEB solution was loaded onto the LFA strip and passed through the absorbent pad. A mixture of antibody-conjugated HGNs and running buffer was then loaded. Antibody-conjugated HGNs subsequently reacted with SEB antigens, thereby forming sandwich immunocomplexes in the test zone. Residual antibody conjugated HGNs were reacted with secondary antibodies immobilized in the control zone. Photographic images of the LFA strips in the presence of different SEB concentrations from 1 ng/mL to 20,000 ng/mL are displayed in Fig. 4a. Red bands were observed in the test zone at SEB concentrations as low as 10 ng/mL. Quantitative analysis was also conducted by recording the optical densities of the test zones with a Chemi-Doc imaging system. In the phase contrast analysis, the limit of detection (LOD) was determined to be 10 ng/mL.

ELISA assays were also performed for SEB antigens. Capture antibodies were immobilized on the surfaces of a 96-well plate, while the remaining sites were treated with BSA to prevent non-specific binding. SEB antigens were then added and bound to the capture antibodies. After washing three times with a micropipette, detecting antibodies were added and bound to the antigens, followed by the addition of enzyme-linked secondary antibodies, which were bound to the detecting antibodies. Finally, a substrate was added and then converted to a detectable form by the enzyme. As shown in Fig. 4b, greater SEB concentrations caused the colour to change from yellow to dark yellow. The LOD determined by the ELISA experiments was estimated to be 1.0 ng/mL.

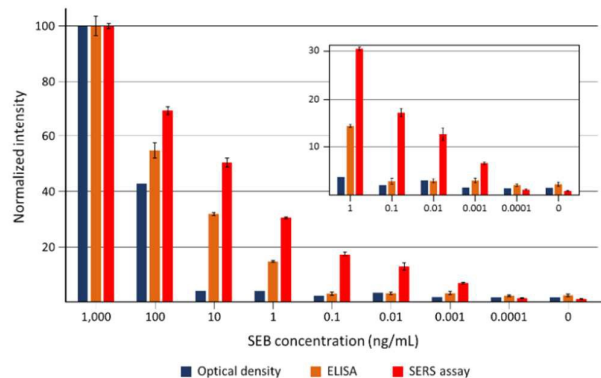


**Fig. 5** Comparison of the assay results obtained with eight different SEB concentrations using the optical density of a POC-based LFA strip, ELISA, and SERS-based LFA strip. The assay results acquired over a low concentration range (0 ~ 1 ng/mL) are displayed in the inset. The error bars indicate standard deviations from three measurements.

Shown in Fig. 5 is a comparison of the SEB assay results obtained with the SERS-based LFA strip, POC-based LFA strip, and ELISA immunoassay kit in the range of  $10^{-4}$  ~  $10^3$  ng/mL. In the SERS-based assay, the Raman peak intensity at  $1615\text{ cm}^{-1}$  was monitored for a quantitative evaluation of the SEB content. Herein, all the values in y-axis for SERS-based assay, ELISA and optical density measurements have been normalized. Detailed data for the normalization are displayed in Table S1. Overall, the values generated by the proposed SERS-based LFA strip are in good agreement with those obtained with the POC-based LFA strip and ELISA assay kit at higher SEB concentrations (over 10 ng/mL). Furthermore, the SERS-based assay results are more consistent in the low concentration range (0 ~ 1 ng/mL) when compared to those recorded by the LFA or ELISA kit, as shown in the inset of Fig. 5. This means that more sensitive quantification of SEB is possible using the devised SERS-based LFA strip. Indeed, the LODs determined from the standard deviations were 10, 1.0, and 0.001 ng/mL for the POC-based LFA strip, ELISA assay kit and SERS-based LFA strip, respectively. All error bars denote the standard deviations from a total of three measurements. Calibration curves for ELISA and SERS-based assays were also determined. Here, a four parameter logistic fitting model has been used to obtain the fitting parameters. The fitting parameters and corresponding calibration curves for ELISA and SERS-based assays are displayed in Fig. S3.

To evaluate the selectivity of the SERS-based strip biosensor, tests were conducted for the same concentration (1,000 ng/mL) of five different toxins: SEB, staphylococcus aureus enterotoxin A (SEA), ochratoxin, aflatoxin, and fumonisin. Photographic images and SERS mapping images of the detection results are displayed in Fig. S4. As expected, the test zone only changed to red in the presence of SEB. In contrast, no obvious color changes were observed for the other toxins. SERS mapping images also demonstrate the same results. Additional tests were conducted for lower concentrations of SEB (500, 100, 50, 10 and 1 ng/mL). Non-specific binding effects were studied for the antigen cocktail solution composed of the five different antigens (SEA, aflatoxin, ochratoxin and fumonisin), with equivalent concentration (100

ng/mL each) of each antigen. Corresponding SERS mapping images are added in Figs. S5a and S5b. The amounts of SEB in cocktail solution mixtures have been quantified via calculations from the calibration fitting curve in Fig. 5a. The assay results for five different concentrations of SEB mixtures showed reasonable accuracy as is shown in Fig. S5c. Such findings demonstrate that our SERS-based strip sensor only responds to SEB and thus, possesses inherently high selectivity.

## Conclusions

In the present study, a novel SERS-based LFA strip was developed for the highly sensitive and rapid detection of SEB in solution. To resolve existing problems associated with LFA strip biosensors (e.g., limits in quantitative analysis and low sensitivity), a SERS-based LFA strip was fabricated in order to conduct SEB assays in a simplified manner. While the measurement principles of the devised sensor are identical to those of a conventional LFA strip, Raman reporter-labelled HGNs were used as SERS detection probes instead of the gold nanoparticles employed in typical LFA sensors. The presence of SEB antigens was confirmed through a colour change in the test zone. Furthermore, a highly sensitive quantitative evaluation of SEB antigens was possible by averaging the SERS mapping signals.

The LOD for the SERS-based LFA strip was estimated to be 0.001 ng/mL. Such a low value is approximately three orders of magnitude more sensitive than that of the corresponding ELISA-based method. Accordingly, the proposed SERS-based LFA strip sensor, which possesses both high sensitivity and quantitative evaluation capabilities, shows significant potential for the rapid and sensitive detection of target markers in a simplified manner.

In addition, we are currently developing a portable Raman system that can be used for POC diagnostics. Using the integrated system composed of a portable Raman spectrometer and a LFA strip, it is expected that a highly accurate quantitative analysis of target biomarkers be achieved in the field. In addition, we are also developing a compact SERS-based immune-analyzer which can provide flexibility and cost-effectiveness to many doctors, clinical labs, hospitals. This Raman reader is a portable Raman scanning instrument for measuring the concentration of target analytes in the human blood, urine and other specimens. We believe that this work takes a step closer to investigating the potential feasibility of SERS-based LFA biosensor for application in POC diagnosis.

## Acknowledgements

The National Research Foundation of Korea supported this work through grant numbers 2008-0061891 and 2009-00426. The Nano Material Technology Development Program also supported this work, through the National Research Foundation of Korea, funded by the Ministry of Science, ICT & Future Planning (2012M3A7B4035288). S.L. acknowledges the

financial support (grant number 2012R1A1A2042550) from the National Research Foundation of Korea.

## Notes and references

- C. Liu, Q. Jia, C. Yang, R. Qiao, L. Jing, L. Wang, C. Xu and M. Gao, *Anal. Chem.*, 2011, **83**, 6778-6784.
- C. Parolo and A. Merkoci, *Chem. Soc. Rev.*, 2013, **42**, 450-457.
- B. B. Dzantiev, N. A. Byzova, A. E. Urusov and A. V. Zherdev, *TrAC, Trends Anal. Chem.*, 2014, **55**, 81-93.
- S. Song, N. Liu, Z. Zhao, E. Njumbe Ediage, S. Wu, C. Sun, S. De Saeger and A. Wu, *Anal. Chem.*, 2014, **86**, 4995-5001.
- B. Kavosi, R. Hallaj, H. Teymourian and A. Salimi, *Biosens. Bioelectron.*, 2014, **59**, 389-396.
- H. Xu, X. Mao, Q. Zeng, S. Wang, A.-N. Kawde and G. Liu, *Anal. Chem.*, 2009, **81**, 669-675.
- X. Gao, H. Xu, M. Baloda, A. S. Gurung, L.-P. Xu, T. Wang, X. Zhang and G. Liu, *Biosens. Bioelectron.*, 2014, **54**, 578-584.
- Y. He, X. Zhang, S. Zhang, M. K. L. Kris, F. C. Man, A.-N. Kawde and G. Liu, *Biosens. Bioelectron.*, 2012, **34**, 37-43.
- H.-A. Joung, Y. K. Oh and M.-G. Kim, *Biosens. Bioelectron.*, 2014, **53**, 330-335.
- J. Yan, Y. Liu, Y. Wang, X. Xu, Y. Lu, Y. Pan, F. Guo and D. Shi, *Sens. Actuator B-Chem.*, 2014, **197**, 129-136.
- D. Yang, J. Ma, Q. Zhang, N. Li, J. Yang, P. A. Raju, M. Peng, Y. Luo, W. Hui, C. Chen and Y. Cui, *Anal. Chem.*, 2013, **85**, 6688-6695.
- M. Blažková, B. Mičková-Holubová, P. Rauch and L. Fukal, *Biosens. Bioelectron.*, 2009, **25**, 753-758.
- G. Posthuma-Trumpie, J. Wichers, M. Koets, L. J. M. Berendsen and A. van Amerongen, *Anal. Bioanal. Chem.*, 2012, **402**, 593-600.
- Q.-Y. Xie, Y.-H. Wu, Q.-R. Xiong, H.-Y. Xu, Y.-H. Xiong, K. Liu, Y. Jin and W.-H. Lai, *Biosens. Bioelectron.*, 2014, **54**, 262-265.
- N. A. Taranova, A. N. Berlina, A. V. Zherdev and B. B. Dzantiev, *Biosens. Bioelectron.*, 2015, **63**, 255-261.
- A. Berlina, N. Taranova, A. Zherdev, Y. Vengerov and B. Dzantiev, *Anal. Bioanal. Chem.*, 2013, **405**, 4997-5000.
- X. Li, D. Lu, Z. Sheng, K. Chen, X. Guo, M. Jin and H. Han, *Talanta*, 2012, **100**, 1-6.
- K. Bobosha, E. M. Tjon Kon Fat, S. J. F. van den Eeden, Y. Bekele, J. J. van der Ploeg-van Schip, C. J. de Dood, K. Dijkman, K. L. M. C. Franken, L. Wilson, A. Aseffa, J. S. Spencer, T. H. M. Ottenhoff, P. L. A. M. Corstjens and A. Geluk, *PLoS Negl. Trop. Dis.*, 2014, **8**, e2845.
- Z. Yan, L. Zhou, Y. Zhao, J. Wang, L. Huang, K. Hu, H. Liu, H. Wang, Z. Guo, Y. Song, H. Huang and R. Yang, *Sens. Actuator B-Chem.*, 2006, **119**, 656-663.
- E. Juntunen, T. Myyryläinen, T. Salminen, T. Soukka and K. Pettersson, *Anal. Biochem.*, 2012, **428**, 31-38.
- G. Rundström, A. Jonsson, O. Mårtensson, I. Mendel-Hartvig and P. Venge, *Clin. Chem.*, 2007, **53**, 342-348.
- Z. Li, Y. Wang, J. Wang, Z. Tang, J. G. Pounds and Y. Lin, *Anal. Chem.*, 2010, **82**, 7008-7014.
- M. D. Porter, R. J. Lipert, L. M. Siperko, G. Wang and R. Narayanan, *Chem. Soc. Rev.*, 2008, **37**, 1001-1011.
- C. I. Brady, N. H. Mack, L. O. Brown and S. K. Doorn, *Anal. Chem.*, 2009, **81**, 7181-7188.
- X. X. Han, L. J. Cai, J. Guo, C. X. Wang, W. D. Ruan, W. Y. Han, W. Q. Xu, B. Zhao and Y. Ozaki, *Anal. Chem.*, 2008, **80**, 3020-3024.
- H. Chon, S. Lee, S. W. Son, C. H. Oh and J. Choo, *Anal. Chem.*, 2009, **81**, 3029-3034.
- M. Lee, S. Lee, J.-h. Lee, H.-w. Lim, G. H. Seong, E. K. Lee, S.-I. Chang, C. H. Oh and J. Choo, *Biosens. Bioelectron.*, 2011, **26**, 2135-2141.

## Journal Name

## ARTICLE

- 28 H. Chon, S. Lee, S.-Y. Yoon, S.-I. Chang, D. W. Lim and J. Choo, *Chem. Commun.*, 2011, **47**, 12515-12517.
- 29 I.-H. Cho., M. Das, P. Bhandaria, and J. Irudayaraja, *Sens. Actuator B-Chem.*, 2015, **213**, 209-214.
- 30 C. E. Talley, J. B. Jackson, C. Oubre, N. K. Grady, C. W. Hollars, S. M. Lane, T. R. Huser, P. Nordlander and N. J. Halas, *Nano Lett.*, 2005, **5**, 1569-1574.
- 31 A. M. Schwartzberg, T. Y. Oshiro, J. Z. Zhang, T. Huser and C. E. Talley, *Anal. Chem.*, 2006, **78**, 4732-4736.
- 32 H. Chon, S. Lee, S.-Y. Yoon, E. K. Lee, S.-I. Chang and J. Choo, *Chem. Commun.*, 2014, **50**, 1058-1060.
- 33 J. Ko, S. Lee, E. K. Lee, S.-I. Chang, L. Chen, S.-Y. Yoon and J. Choo, *Phys. Chem. Chem. Phys.*, 2013, **15**, 5379-5385.
- 34 K. Dutta, A. K. Varshney, M. C. Franklin, M. Goger, X. Wang and B. C. Fries, *J. Biol. Chem.*, 2015, **290**, 6715-6730.
- 35 M. Larena, J. Holmgren, M. Lebens, M. Terrinoni and A. Lundgren, *J. Immunol.*, 2015, **194**, 3829-3839.